Published in final edited form as:
Ultrasound Med Biol. 2007 April ; 33(4): 576–583.

DUTY CYCLE DEPENDENCE OF ULTRASOUND ENHANCED THROMBOLYSIS IN A HUMAN CLOT MODEL

Jason M. Meunier[*], **Christy K. Holland**[†,‡], **Christopher J. Lindsell**[*], and **George J. Shaw**[*,†,§]

***** *Department of Emergency Medicine, College of Medicine, University of Cincinnati, Cincinnati, OH, USA*

† *Department of Biomedical Engineering, College of Medicine, University of Cincinnati, Cincinnati, OH, USA*

‡ *Department of Radiology, College of Medicine, University of Cincinnati, Cincinnati, OH, USA*

§ *Greater Cincinnati/Northern Kentucky Stroke Team, College of Medicine, University of Cincinnati, Cincinnati, OH, USA*

Abstract

Combined ultrasound and tissue plasminogen activator (rt-PA) therapy, or ultrasound enhanced thrombolysis (UET), has been shown to improve recanalization in patients with acute ischemic stroke. We measured the effect of ultrasound duty cycle on the lytic efficacy of 120 kHz UET in an *in vitro* human clot model. The hypothesis was that an increase in duty cycle increases rt-PA lytic efficacy. Human whole blood clots were exposed to 120-kHz ultrasound and rt-PA for 30 min in human plasma. The duty cycle ranged from 0% to 80%, where 0% represents sham exposure. Clot lytic rate was measured by recording the clot width over time. The clot width after 30 min exposure to rt-PA and ultrasound decreases with increasing duty cycle. The initial lytic rate increased linearly with duty cycle.

Keywords

Ultrasound enhanced thrombolysis; Duty cycle; Tissue plasminogen activator; Human whole blood clot

INTRODUCTION

The majority of strokes (~80%) are ischemic in origin, caused either by embolic events or *in situ* thrombosis (Adams et al. 1996). The only treatment for ischemic stroke currently approved by the FDA is IV delivered recombinant tissue plasminogen activator (rt-PA). The clot occluding the blood vessel can be lysed using rt-PA, leading to recanalization. However, rt-PA has significant side effects, including intracranial hemorrhage (ICH). Thus, the development of adjunctive therapies, such as ultrasound-enhanced thrombolysis (UET), is under investigation. Recently, 2 MHz transcranial ultrasound was shown to increase the efficacy of rt-PA and to decrease the probability of incomplete thrombolysis (Alexandrov et al. 2004a, 2004b). However, other studies using 300-kHz transcranial ultrasound have shown no increase in rt-PA lytic efficacy and an increased ICH rate in acute ischemic stroke patients (Daffertshofer et al. 2005). It is clear the “optimal” ultrasound parameters for UET have not yet been identified.

Address correspondence to: Jason M. Meunier, University of Cincinnati, Department of Emergency Medicine, 231 Albert Sabin Way, PO Box 670769, Cincinnati, OH 45267-0769, USA. E-mail: meuniejn@uc.edu

Optimization of ultrasound parameters is necessary to improve UET as a potential therapy for ischemic stroke. For example, it is known that ultrasound with a lower frequency (120 kHz) penetrates the temporal bone with less attenuation than a higher frequency (1 MHz) (Coussios et al. 2002). An additional parameter of ultrasound is the duty cycle, the percentage of time during which the ultrasound signal is "on." In this study, we measure the effects of varying duty cycle on 120 kHz UET in an *in vitro* human clot model. The hypothesis was that an increase in duty cycle increases the ultrasound enhancement of rt-PA thrombolysis.

MATERIALS AND METHODS

Preparation of rt-PA and human plasma

The rt-PA was obtained as a lyophilized powder (rt-PA, Activase, Genentech, San Francisco, CA, USA). The powder was mixed with sterile water to a concentration of 1 mg/mL, as per manufacturer's instructions, then immediately aliquoted into 1.0 mL centrifuge tubes (Fisher Scientific) and stored at −70°C. The enzymatic activity of rt-PA is stable for at least 1 y when stored in this fashion (Jaffe et al. 1989). Human fresh-frozen plasma (hFFP) was obtained from a local blood bank. One unit contains approximately 250 mL of plasma. Each unit was briefly thawed to the liquid state, aliquoted into 50 mL centrifuge tubes (Fisher Scientific) and then immediately stored at −70°C. Individual aliquots of rt-PA and plasma were allowed to thaw for subsequent experiments and unused portions were discarded following completion of the experiment.

Production of sample clots

Human whole blood was drawn from six volunteers by sterile venipuncture following local Institutional Review Board approval. Volume samples of 1 to 2 mL were placed in sterile glass tubes (Vacutainer) and allowed to form clots in a small diameter (~600 μm) micropipette (Becton, Dickinson and Co., Franklin Lakes, NJ, USA; 20λ) through which a short segment of 7-0 silk suture (Ethicon Industries, Cornelia, GA, USA) had been threaded. This is similar to clot production methods used in imaging studies by Winter et al. (2005) and Yu et al. (2000).

The clots were incubated for 3 h at a temperature of 37°C and refrigerated at 5°C for 3 d for maximal clot retraction, lytic resistance and stability (Francis and Totterman 1995;Loren et al. 1989;Shaw et al. 2006). The reason for this aging process is that there is a clot age effect in the response of whole blood clots to lytic agents. For example, Emelianov et al. (2002) found that the "Young's modulus," which is a measure of mechanical stiffness, increased substantially over several days, in an *in vitro* rat model. Similarly, Francis et al. (1995) found that the clinical response to lytic therapy in deep venous thrombosis was greater in clots less than 4 d of age than in patients with more prolonged symptoms. Shaw et al. (2006) similarly observed that whole blood clots less than 3 d old were less resistance to rt-PA lysis than more aged clots. For these reasons, the sample clots in this work were incubated for 3 d, (1) to avoid any clot aging effects in their response to rt-PA and (2) to maximize the lytic resistance of the whole blood clots.

Before each experiment, the micropipette was removed to produce a thin cylindrical clot adherent to the 7-0 suture; this clot was typically 5 to 8 μl in volume and less than 300 μm in width (see Fig. 1). At this size the clots were similar in diameter to the intracerebral segments of the middle cerebral arteries (80 to 840 μm in diameter) or other cerebral vessels such as the recurrent artery of Heubner and its perforators (643 ± 237 μm in diameter) (Marinkovic et al. 1985;Tao et al. 2006).

Visualization of the clot

For each experiment, the sample clot was placed in a clean 2-mm diameter micropipette (Drummond Scientific Co., Broomall, PA, USA; 200 μL) and inserted into a U-shaped sample holder composed of hollow Luer lock connectors and silicone tubing (Cole Parmer, Vernon Hills, IL, USA; outer diameter 0.125 in., 3.18 mm). The sample holder was then placed in a water-filled acrylic tank with a microscope slide window at the bottom (Fig. 2). A custom-made 120 kHz ultrasound transducer (Sonic Concepts Inc, Woodburn, WA, USA) was placed at one end of the tank. This transducer was calibrated using a PVDF hydrophone (Reson, Goleta, CA, USA; TC4038). The −6 dB beam width was found to be 1.0 cm with a focal length of 3.2 cm. In these experiments, the transducer was mounted within the tank at an angle of 30° with respect to the bottom of the tank. The acoustic pressure attenuation by the micropipette tubing was found to be less than 1% (Cheng et al. 2005). Sound absorbing material (rho-c rubber) was placed at the opposite end of the tank to inhibit acoustic standing waves. Water in the tank was maintained at a temperature of 37 ± 1°C for all experiments by using a small heating element (Hagen, Mansfield, MA, USA; 50 W). The tank was placed over the objective of an inverting microscope (Olympus, Melville, NY, USA; IM) and the full width of the clot visualized. The field-of-view of the image is approximately 340 μm × 260 μm (640 pixels × 480 pixels). The apparatus was placed on top of a vibration isolation table (Newport, Irvine, CA, USA; XL-G) to minimize motion artifacts during data acquisition times of approximately 30 min. Images were recorded at a rate of six frames per min using a CCD camera (Hitachi, Woodbury, NY, USA; KP-M1A). Data were stored for later analysis on a computer (Dell, Round Rock, TX, USA; Intel Pentium). A complete description of the clot imaging apparatus has been provided by Cheng et al. (2005).

Experiment protocol

Following placement of the sample holder in the tank, a sample clot was exposed to one of three regimens: these were (1) hFFP alone (control); (2) hFFP and rt-PA ([rt-PA] = 3.15 μg/mL) (sham); or (3) hFFP, rt-PA and ultrasound (treatment). This rt-PA concentration was chosen to be well within the therapeutic concentration range in humans (Siefried et al. 1989; Tanswell et al. 1991). Individual trials began by slowly injecting approximately 1 mL of hFFP (control trials) or hFFP and rt-PA (sham and treatment trials) into the U-shaped sample holder with a 1 mL syringe. At time equal to zero, t = 0, the solution was in full contact with the clot. Removing the syringe following injection exposed the ends of the sample holder to atmospheric pressure and the clot surface to a static fluid column (Cheng et al. 2005). Ultrasound of 120 kHz was provided *via* the transducer at one end of the tank. Each clot treated with ultrasound was exposed to 120 kHz ultrasound with a peak-to-peak pressure amplitude of 0.35 $MPa_{p\text{-}p}$ and a pulse repetition frequency (PRF) of 1667 Hz. The duty cycle was 10%, 20%, 50% or 80%; the average spatial intensity at each duty cycle is 0.43, 0.85, 2.1 and 3.4 W/cm^2, respectively. At least five clots (mean = 8, range = 5 to 10) were used in each regimen. Clots from at least two donors were used for each regimen (control, sham and individual duty cycle treatment groups).

Determination of lysis

Light transmission through the clot depends on the amount of clot traversed and the clot density (Cheng et al. 2005). Figure 3a shows a schematic of light transmission in this experiment through the cross-section of a sample cylindrical clot of radius R. Light is incident from the top of the clot along the y-axis, transmitted through the clot thickness and is received by the microscope objective at the bottom. (A typical example of the resulting image is shown in Fig. 3b). Note that, in this diagram, at each value of x (the horizontal axis, across the width of the clot), the total clot thickness that the light traverses is

$$L(x) = 2T(x) = 2(R^2 - x^2)^{1/2} \quad (1)$$

If the light intensity at x is denoted I(x), then using the Beer-Lambert law for light absorption through media yields an expression for I(x) (Sassaroli and Fantini 2004),

$$I(x) = I_o e^{-\mu L(x)} \quad (2)$$

and substituting for L(x) yields

$$\frac{I(x)}{I_o} = e^{-2\mu\sqrt{R^2 - x^2}} \quad (3)$$

where μ (a constant) is the clot light absorption coefficient, and I_o is the incident light intensity.

Figure 4 exhibits the normalized light intensity (I/I_o; line of circles) as a function of x for a sample clot at a fixed value of z. The solid line is a fit to eqn 3, yielding r = 174 μm, and the agreement is quite good ($R^2 = 0.98$). The discontinuity in (I/I_o) in the clot center is the suture and this region is not included in the fit. The correspondence of the cylindrical clot model to the transverse light intensity profile implies that the approximate morphology of the sample clots is cylindrical, as shown schematically in Figs. 1 and 3a. Therefore, the imaged clot width corresponds to the sample clot diameter.

Using light transmission, the edges of the clots can be identified and used to determine average clot width. To accomplish this, the image light intensity $I(x, z)$ was recorded using the CCD camera; the intensity data at each pixel in a given frame was digitized and stored as a function of (x, z). The clot width was then calculated, using a computer program written in Matlab 6.5 R13 (Mathworks, Inc., Natwick, MA, USA). First, the spatial gradient of the light intensities $\partial I(x,z)/\partial X$ was calculated for each row (fixed z) of pixels. The positions of the two clot-plasma interfaces were determined *via* an edge-detection routine that finds the values of $x = (x_1, x_2)$ for each z such that $\partial II\partial x(x_{1,2},z) \geq \Gamma$, where Γ is a constant. A Γ of 2.5 is sufficient to detect well-defined clot edges. The width W(z) of the clot at each z was then $w(z) = |x_1 - x_2|$. The average clot width was calculated by averaging the width over all z values in each image and then normalizing by the clot width at time t = 0. Thus, the average clot width could be tracked over time with this unique clot treatment postprocessing scheme for each regimen (control, sham and treatment groups). The clot width after 30 min was also used for comparing the effects of thrombolysis between groups.

Statistical analysis

The effects of duty cycle on normalized average clot width were evaluated using a mixed-model analysis of variance. This method of analysis allows one to estimate the fixed effects of the various treatments while appropriately modeling the covariance structure arising from the within subject design. Data are presented as mean values with standard deviations, unless explicitly stated otherwise. Parameter estimates and standard errors of the parameter estimates are used to report the effects of ultrasound and rt-PA. These calculations were performed using SAS v8.02 (SAS Institute, Cary, NC, USA) and a p value of less than 0.05 was considered to be significant.

RESULTS

Figure 5 shows an example of a clot exposed to ultrasound (0.35 $MPa_{p\text{-}p}$, 50% duty cycle) and rt-PA after 1 and 7 min, respectively. In Fig. 5a, the clot is shown before any measurable lysis. The clot extends across the field-of-view, and both clot edges are visible. Figure 5b shows the

sample clot after 7 min and the width of the clot has been greatly reduced due to lysis. Both edges of the clot are still visible, but sufficient clot lysis has occurred such that the smooth edge on the left of the lysed clot reveals the suture around which the clot originally formed. Degradation products are also visible in the plasma to either side of the clot.

Figure 6 shows the normalized average clot width as a function of time for control, rt-PA (sham) and ultrasound plus rt-PA (treatment) trials; the solid vertical bars are representative standard deviations for the normalized data. The clot width for sham and 10% duty cycle treatment trials are very similar for the entire 30 min of UET exposure. As duty cycle is increased to 20%, a greater degree of lysis occurs; as duty cycle is increased to 50% and 80%, the clot width decreases further in response. The change in clot width in control trials is very similar in magnitude to the change in clot width for 10% duty cycle treatment trials. Note that the vertical bars indicate representative standard deviations for the normalized clot width data for each duty cycle.

In six cases, the clot was completely lysed by the combination of rt-PA and ultrasound within the 30 min exposure period. Instances of complete clot dissolution are noted by vertical arrows in Fig. 6, which mark the time of dissolution and the appropriate trial group: one, two and three clots were completely dissolved in the 20%, 50% and 80% duty cycle treatment groups, respectively. There were no instances of clot dissolution in control, rt-PA alone and 10% duty cycle treatment groups. The mean dissolution time for all trials was 11.0 ± 3.84 min. For treatment groups, the mean dissolution time is 10.0 min (20% duty cycle), 15.2 ± 1.18 min (50% duty cycle) and 8.56 ± 3.06 min (80% duty cycle). Again, dissolution does not happen for all of the sample clots, but it does seem to occur with increasing frequency for the higher duty cycles. With an average initial clot width of 240 μm, the normalized clot width following clot dissolution is 0.26 mm on average.

The normalized average clot width as a function of time can be approximated by a least squares fit to the equation

$$\Lambda(t) = B + (1 - B)e^{-kt} \tag{4}$$

where Λ is the normalized average clot width (dimensionless), B is the final value of the normalized average clot width (also dimensionless) and k is the exponential decay rate constant (min^{-1}). The solid line of Fig. 6 shows the corresponding curve fit for the treatment group in which clots were exposed to rt-PA and 80% duty cycle ultrasound. The quality of the fits is demarcated by R^2, which is greater than or equal to 0.87 for all trials.

As shown in Fig. 6, normalized average clot width in most UET-treated trials not only achieves a lower value than in sham trials, leading to smaller values of the clot diameter after 30 min, but, qualitatively, the clot diameter appears to decrease more rapidly as duty cycle increases. The duty cycle-dependence of the initial lytic rate (LR) can be studied using the exponential decay model. For small values of time t, eqn 4 can be approximated by

$$\Lambda(t) \approx 1 - (1 - B)kt \tag{5}$$

where Λ is the normalized average clot width, B is the final value of the normalized average clot width and k is the lytic rate constant, as described previously. Using this relationship, the initial lytic rate (LR) can be defined as

$$LR = (1 - B)k \tag{6}$$

As shown in Fig. 7, values for the initial lytic rate increase as duty cycle increases. The initial lytic rate for clots exposed to ultrasound with a duty cycle of 80% is nine times that of clots

exposed to rt-PA alone (0% duty cycle). Also, the initial lytic rate is linear for all duty cycles (using a least-squares fit to the data; $R^2 = 0.99$).

DISCUSSION

It has been shown that the lytic efficacy of 120 kHz UET increases with increasing duty cycle in this *in vitro* human clot model. The normalized average clot width was found to be well-described by a simple two-parameter exponential decay model. In addition, the normalized average clot width after 30 min of exposure to ultrasound and rt-PA is much smaller at a duty cycle of 20% or greater than following exposure to rt-PA alone or rt-PA with 10% duty cycle ultrasound. To our knowledge, this is the first report measuring the lytic efficacy of UET on reducing the physical dimensions of human clot. Reducing the size and eliminating the obstructive thrombus is the primary clinical goal in treating thrombotic disease, such as ischemic stroke.

The ability of ultrasound to enhance the lytic efficacy of rt-PA has been demonstrated both *in vivo* and *in vitro* by others (Alexandrov et al. 2004a;Blinc et al. 1993;Suchkova et al. 2002). There are many possible mechanisms for this enhancement, including heating, acoustic streaming, increased permeation of rt-PA into the clot and cavitation (Blinc et al. 1993;Francis et al. 1995;Sakharov et al. 2000;Polak 2004;Schäfer et al. 2005;Frenkel et al. 2006) or combinations thereof. Recently, Datta et al. (2006) measured the induction of stable cavitation in porcine whole blood clots in porcine plasma. Sample clots were exposed to rt-PA, 120 kHz ultrasound (80% duty cycle), or both. This group determined that the minimum peak-to-peak pressure resulting in stable cavitation in porcine clots exposed to rt-PA, plasma and 120 kHz ultrasound was 0.4 ± 0.04 MPa, close to the value of 0.35 MPa used in these experiments using human plasma and whole blood clots. It is possible that cavitation, either inertial or stable or both, is a contributor to the ultrasonic enhancement of rt-PA efficacy observed here. Further, if the predominant mechanism is cavitation, then a linear duty cycle dependence is quite plausible. In such a mechanism, the cavitating bubbles exist primarily during the period of the actual ultrasound signal. Therefore, increasing the duty cycle could increase the duration of these bubbles in a proportional manner, particularly for stable cavitation. It must be pointed out that this proposed mechanism is speculative.

Although others have measured an increase in UET with increasing duty cycle; our observation of a linear dependence has not previously been seen. In the elegant work of Suchkova et al. (2002), percent clot lysis was measured for several ultrasound frequencies and parameters. In their work, plasma clots were made from citrated human plasma and exposed to rt-PA and ultrasound. Clot lysis was measured by determining the percent of solubilized fibrin from the sample clot. Their duty cycles ranged from 1% to 100% (CW) and the ultrasound intensity was a maximum of 1 W/m^2; this value roughly corresponds to a 0.17 MPa peak-to-peak pressure. This is substantially less than the stable cavitation threshold of 0.4 ± 0.04 MPa as measured by Datta et al. (2006) and much less than previously reported cavitation thresholds in tissue measured by Coleman et al. (1995). It may be possible that mechanisms other than cavitation were responsible for the enhanced clot lysis observed by this group, whereas we tentatively propose that cavitation may be the mechanism responsible for UET in the present experiments.

While the duty-cycle-dependent enhancement in the initial lytic rate suggested by results of other studies has been illustrated here *in vitro*, the novelty of this work is that we directly demonstrate the efficacy of UET in reducing the physical size of the sample clot. Clot size is arguably the most important parameter for clinical intervention and its direct measurement gives important information relevant to lytic therapy. The increased rate of thrombus reduction arising from increasing duty cycle possibly implies an increased rate of recanalization *in vivo*, which in turn has implications toward patient improvement (Ishibashi et al. 2002;Molina

et al. 2006). In patients receiving IV rt-PA, Alexandrov et al. (2001) showed that more rapid recanalization of an obstructed cerebral artery predicted better short-term patient outcome. Similarly, Molina et al. (2004) noted that the degree of recanalization within 300 min of rt-PA treatment was a predictor of patient outcome at three months. Patients with complete or partial recanalization following treatment with rt-PA had better long-term outcomes; a lack of early recanalization was predictive of poorer long-term outcome (Labiche et al. 2003;Molina et al. 2004;Ribo et al. 2004). The results of this study, the first report on effects of UET on the physical dimensions of a clot *in vitro*, suggest that optimization of ultrasound parameters such as duty cycle could improve the potential combination thrombolytic therapies using UET.

SUMMARY

This study confirms our hypothesis that human whole blood clots exposed to plasma, rt-PA and pulsed 120 kHz ultrasound *in vitro* demonstrate an increase of lytic efficacy with increasing duty cycle. This is evidenced by the increase in the initial lytic rate and the overall decrease in normalized average clot width with increasing duty cycle in UET treated clots. The substantial increase in initial lytic rate as duty cycle increases may imply improved early recanalization in the *in vivo* and clinical settings. Further work is needed to optimize UET for potential clinical applications, such as acute ischemic stroke treatment.

Acknowledgements

The authors gratefully acknowledge the support of the Whitaker Foundation (biomedical engineering research grant RG-01-0218) and the National Institutes of Health (NIH/NINDS K02-NS056253).

References

Adams HP, Brott TG, Furlan AJ, et al. Guidelines for thrombolytic therapy for acute stroke. Stroke 1996;27:1711–1718. [PubMed: 8784157]

Alexandrov AV, Burgin WS, Demchuk AM, El-Mitwalli A, Grotta JC. Speed of intracranial clot lysis with intravenous tissue plasminogen activator therapy: Sonographic classification and short-term improvement. Circulation 2001;103:2897–2902. [PubMed: 11413077]

Alexandrov AV, Demchuk AM, Burgin WS, et al. Ultrasound-enhanced thrombolysis for acute ischemic stroke: Phase I. Findings of the CLOTBUST trial. J Neuroimaging 2004;14:113–117. [PubMed: 15095555]

Alexandrov AV, Molina CA, Grotta JC, et al. Ultrasound-enhanced systemic thrombolysis for acute ischemic stroke. N Engl J Med 2004;351:2170–2178. [PubMed: 15548777]

Blinc A, Francis CW, Trudnowski JL, Carstensen EL. Characterization of ultrasound-potentiated fibrinolysis *in vitro*. Blood 1993;81:2636–2643. [PubMed: 8490172]

Cheng JY, Shaw GJ, Holland CK. *In vitro* microscopic imaging of enhanced thrombolysis with 120-kHz ultrasound in a human clot model. ARLO 2005;6:25–29.

Coleman AJ, Kodama T, Choi MJ, Adams T, Saundes JE. The cavitation threshold of human tissue exposed to 0.2 MHz pulsed ultrasound: Preliminary measurements based on a study of clinical lithotripsy. Ultrasound Med Biol 1995;21:405–417. [PubMed: 7645132]

Coussios CC, Holland CK, Shaw GJ. Transmission of a large unfocussed 120 kHz and 1 MHz ultrasound beam through the human skull. J Acoust Soc Am 2002;112:2433.

Daffertshofer M, Gass A, Ringleb P, et al. Transcranial low-frequency ultrasound-mediated thrombolysis in brain ischemic: Increased risk of hemorrhage with combined ultrasound and tissue plasminogen activator-Results of a phase II clinical trial. Stroke 2005;36:1441–1446. [PubMed: 15947262]

Datta S, Coussios C, McAdory LE, et al. Correlation of cavitation with ultrasound enhancement of thrombolysis. Ultrasound Med Biol 2006;32:1257–1267. [PubMed: 16875959]

Emelianov SY, Chen X, O'Donnell M, et al. Triplex ultrasound: Elasticity imaging to age deep venous thrombosis. Ultrasound Med Biol 2002;28:757–767. [PubMed: 12113788]

Francis CW, Blinc A, Lee S, Cox C. Ultrasound accelerates transport of recombinant tissue plasminogen activator into clots. Ultrasound Med Biol 1995;21:419–424. [PubMed: 7645133]

Francis CW, Totterman S. Magnetic resonance imaging of deep vein thrombi correlates with response to thrombolytic therapy. Throm Haemost 1995;73:386–391.

Frenkel V, Oberoi J, Stone MJ, et al. Pulsed high-intensity focused ultrasound enhances thrombolysis in an *in vitro* model. Radiology 2006;239:86–93. [PubMed: 16493016]

Ishibashi T, Akiyama M, Onoue H, Abe T, Furuhata H. Can transcranial ultrasonication increase recanalization flow with tissue plasminogen activator? Stroke 2002;33:1399–1404. [PubMed: 11988621]

Jaffe GJ, Green GD, Abrams GW. Stability of recombinant tissue plasminogen activator. Am J Ophthalmol 1989;108:90–91. [PubMed: 2502019]

Labiche LA, Al-Senani F, Wojner AW, et al. Is the benefit of early recanalization sustained at three months? A prospective cohort study. Stroke 2003;34:695–698. [PubMed: 12624293]

Loren M, Garcia Frade LJ, Torrado MC, Navarro JL. Thrombous age and tissue plasminogen activator mediated thrombolysis in rats. Thromb Res 1989;56:67–76. [PubMed: 2512687]

Marinkovic SV, Milisavljevic MM, Kovacevic MS, Stevic ZD. Perforating branches of the middle cerebral artery: Microanatomy and clinical significance of their intracerebral segments. Stroke 1985;16:1022–1029. [PubMed: 4089920]

Molina CA, Alexandrov AV, Demchuk AM, et al. Improving the predictive accuracy of recanalization on stroke outcome in patients treated with tissue plasminogen activator. Stroke 2004;35:151–156. [PubMed: 14671245]

Molina CA, Ribo M, Rubiera M, et al. Microbubble administration accelerates clot lysis during continuous 2-MHz ultrasound monitoring in stroke patients treated with intravenous tissue plasminogen activator. Stroke 2006;37:425–429. [PubMed: 16373632]

Polak JF. Ultrasound energy and the dissolution of thrombus. N Engl J Med 2004;351:2154–2155. [PubMed: 15548774]

Ribo M, Garami Z, Uchino K, et al. Detection of reversed basilar flow with power-motion Doppler after acute occlusion predicts favorable outcome. Stroke 2004;35:79–82. [PubMed: 14671244]

Sakharov DV, Hekkenberg RT, Rijken DC. Acceleration of fibrinolysis by high frequency ultrasound: The contribution of acoustic streaming and temperature rise. Thromb Res 2000;100:333–340. [PubMed: 11113277]

Sassaroli A, Fantini S. Comment on the modified Beer-Lambert law for scattering media. Phys Med Biol 2004;49:N255–N257. [PubMed: 15357206]

Schäfer S, Kliner S, Klinghammer L, et al. Influence of ultrasound operating parameters on ultrasound-induced thrombolysis *in vitro*. Ultrasound Med Biol 2005;31:841–847. [PubMed: 15936499]

Seifried E, Tanswell P, Ellbruck D, Haerer W, Schmidt A. Pharmacokinetics and haemostatic status during consecutive infusion of recombinant tissue-type plasminogen activator in patients with acute myocardial infarction. Thromb Haemostat 1989;61:497–501.

Shaw GJ, Bavani N, Dhamija A, Lindsell CJ. Effect of mild hypothermia on the thrombolytic efficacy of 120 kHz ultrasound enhanced thrombolysis in an *in vitro* human clot model. Thromb Res 2006;117 (5):603–608. [PubMed: 15951005]

Suchkova V, Carstensen EL, Francis CW. Ultrasound enhancement of fibrinolysis at frequencies of 27 to 100 kHz. Ultrasound Med Biol 2002;28:377–382. [PubMed: 11978418]

Tanswell P, Seifried E, Stang E, Krause J. Pharmacokinetics and hepatic catabolism of tissue-type plasminogen activator. Arzneim-Forsch/Drug Res 1991;12:1310–1319. [PubMed: 1815534]

Tao X, Yu XJ, Bhattarai B, et al. Microsurgical anatomy of the anterior communicating artery complex in adult Chinese heads. Surg Neurol 2006;65:155–161. [PubMed: 16427412]

Winter PM, Shukla HP, Caruthers SD, et al. Molecular imaging of human thrombus with computed tomography. Acad Radiol 2005;12 (Suppl 1):S9–S13. [PubMed: 16106538]

Yu X, Song SK, Chen J, et al. High-resolution MRI characterization of human thrombus using a novel fibrin-targeted paramagnetic nano-particle contrast agent. Magn Reson Med 2000;44:867–872. [PubMed: 11108623]

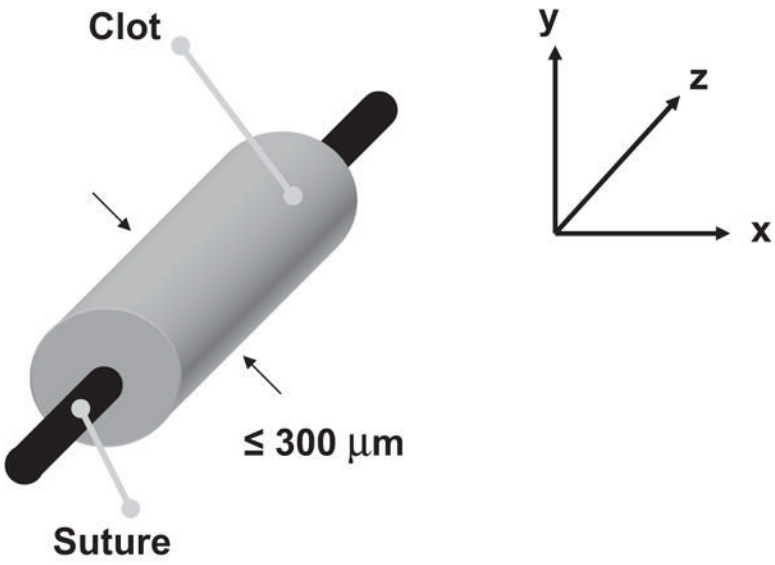

Fig 1.

Typical sample blood clot orientation for this study. Using a 20 μl micropipette and a 7-0 suture, a blood clot with a volume of approximately 5–8 μl is created. The clot is approximately 300 μm in width, allowing it to be visualized completely within the field-of-view of the microscope using a 40× objective.

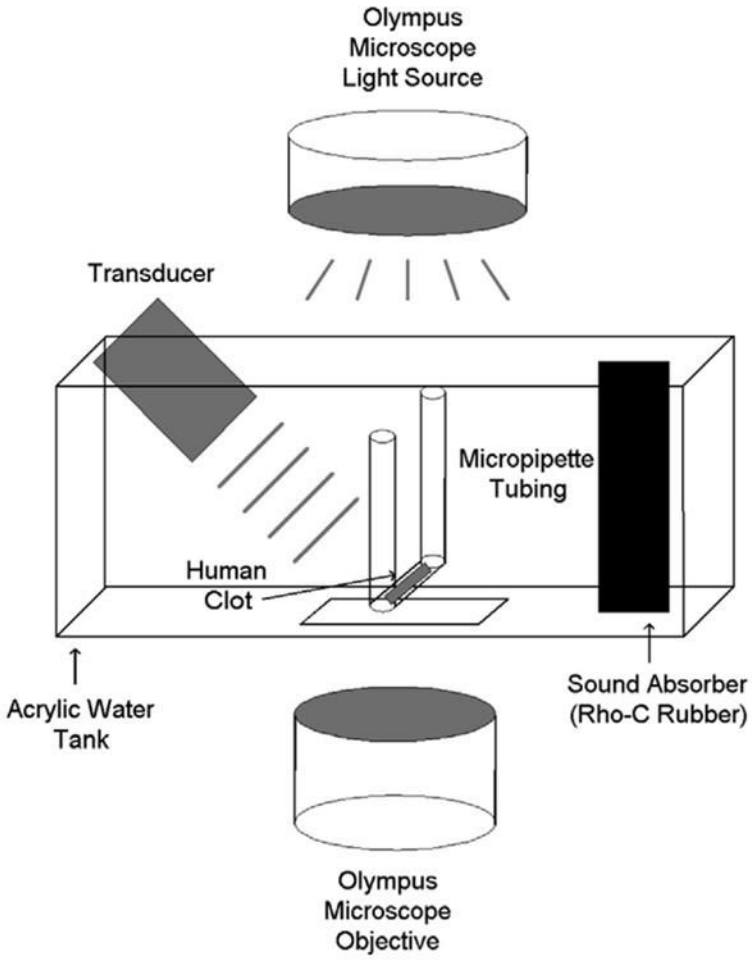

Fig 2.

Apparatus used for *in vitro* ultrasound enhanced thrombolysis experiments. The human whole blood clot is contained in hollow tubing, which is placed within an acrylic tank filled with water at a temperature of 37°C. The tank is situated over a microscopic objective, allowing visualization. An ultrasound transducer is aligned at one end of the tank, and a sound absorbing material is at the opposite end.

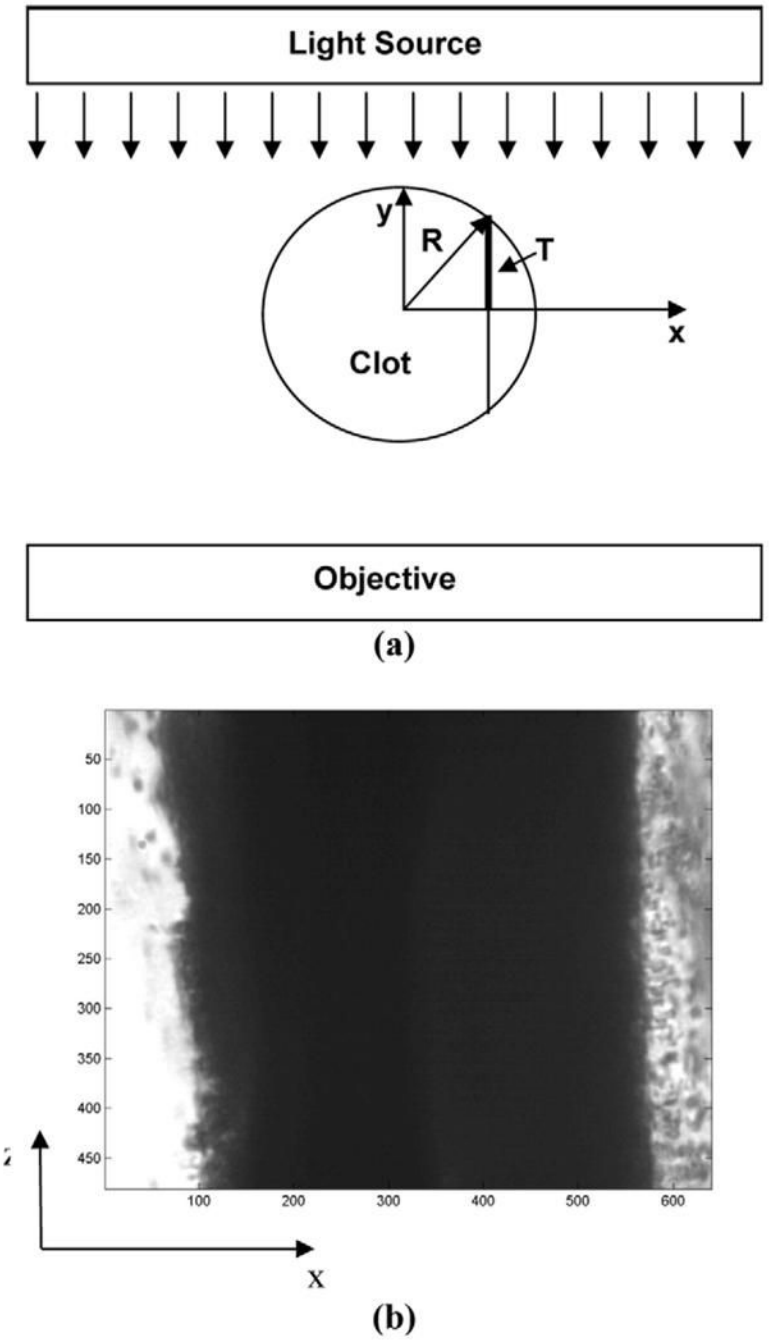

Fig 3.

Illustration of image formation of a cylindrical clot. (a) The light source, clot, and microscope objective are shown in cross-section in the x-y plane. Light (parallel downward arrows) is transmitted through the clot and reaches the microscope objective below. The total clot thickness at any location on the x-axis is $2T(x) = 2(R^2 - x^2)^{1/2}$ (eqn 1). (b) The clot, shown in the x-z plane, is visualized along its length through the objective. The numbers along the x and z axes denote pixel number and one pixel is roughly equivalent to 0.5 μm.

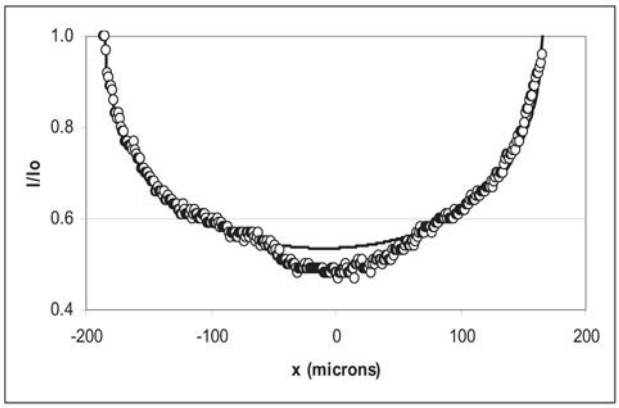

Fig 4.

Light intensity I(x) vs. x in a sample clot. The transverse light intensity (I) profile of a sample clot at a fixed value of z has been normalized to the average light intensity (I_o) in the plasma, indicated by the line of circles (○). The x-axis is the distance from the clot center in μm. The solid line is a fit to the data of Eqn 3 ($R^2 = 0.98$).

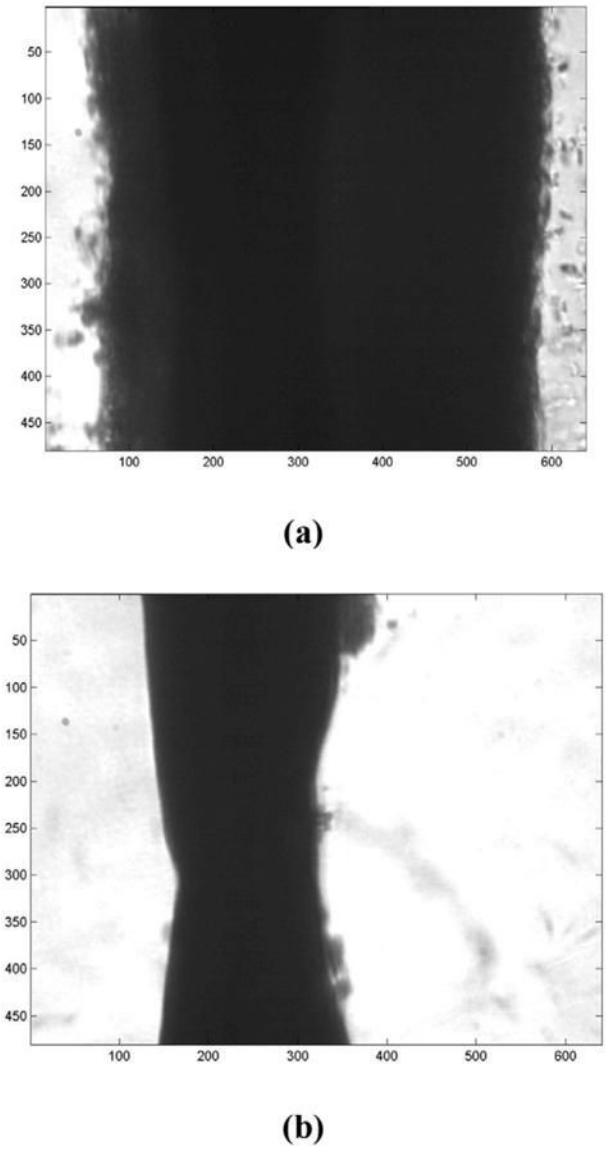

Fig 5.

Photomicrograph of a human whole blood clot. (a) The clot is shown after 1 min of exposure to rt-PA and 120 kHz ultrasound treatment with a duty cycle equal to 50%. As in Fig. 3, the numbers along the x and z axes denote pixel number and one pixel is roughly equivalent to 0.5 μm. Note that the plasma-clot interfaces are well-defined. (b) The clot is shown after 7 min of exposure. Substantial thrombolysis has occurred, and the clot is mostly degraded. Note the degradation products evident in the plasma.

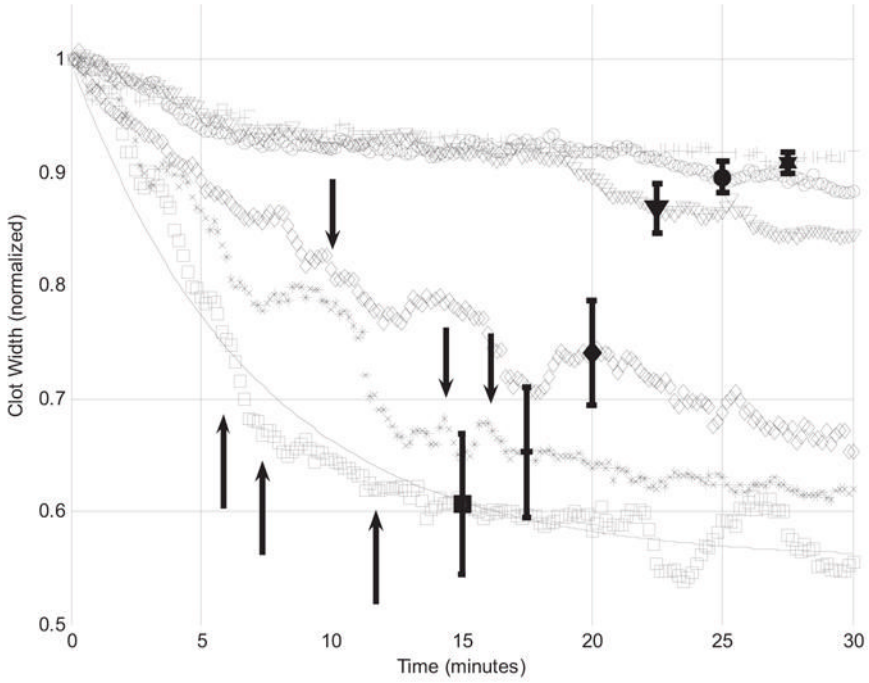

Fig 6.

Normalized average clot width vs. time for clots exposed to ultrasound enhanced thrombolysis at different duty cycles. Normalized average clot width is shown for control (+), sham ([inverted triangle]) and treatment trials with duty cycles of 10 (open circle), 20 (open diamond), 50 (asterisk) or 80% (open square). Vertical bars show standard deviations. The solid line is a best-fit curve, using eqn 4, to clots exposed to rt-PA and 80% duty cycle ultrasound. Black vertical arrows mark incidences of clot dissolution.

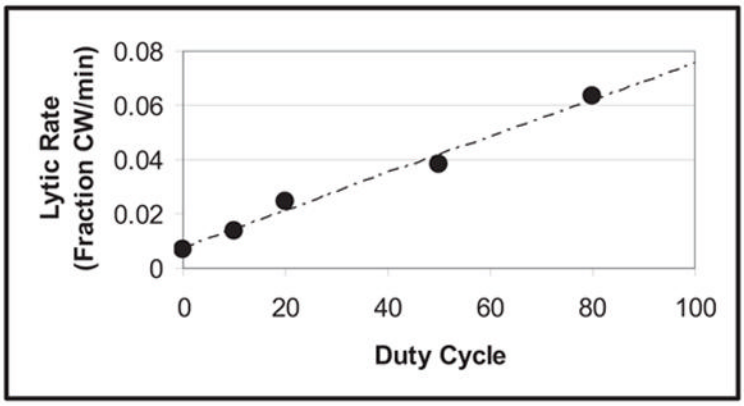

Fig 7.

The initial lytic rate vs. duty cycle for 120 kHz ultrasound enhanced thrombolysis. The initial lytic rate (filled circle) shown for each duty cycle is determined from eqn 6. The lytic rate increases in a linear fashion with increases in duty cycle. The dashed line is a fit to the data (R^2 = 0.99).